

# Generation properties of coherent infrared radiation in the optical absorption region of GaSe crystal

Ching-Wei Chen, Yu-Kuei Hsu, Jung Y. Huang, and Chen-Shiung Chang

Department of Photonics and Institute of Electro-Optical Engineering, National Chiao Tung University, Hsinchu, Taiwan 30010, R.O.C.

[cwchen.eo90g@nctu.edu.tw](mailto:cwchen.eo90g@nctu.edu.tw), [ykhsueo@gmail.com](mailto:ykhsueo@gmail.com), [cschang@mail.nctu.edu.tw](mailto:cschang@mail.nctu.edu.tw), [jyhuang@cc.nctu.edu.tw](mailto:jyhuang@cc.nctu.edu.tw)

Jing-Yuan Zhang

Department of Physics, Georgia Southern University, Statesboro, GA 30460, USA.

[jy Zhang@georgiasouthern.edu](mailto:jy Zhang@georgiasouthern.edu)

Ci-Ling Pan

Department of Photonics and Institute of Electro-Optical Engineering, National Chiao Tung University, Hsinchu, Taiwan 30010, R.O.C.

[clpan@faculty.nctu.edu.tw](mailto:clpan@faculty.nctu.edu.tw)

**Abstract:** We report a study of the effect of optical absorption on generation of coherent infrared radiation from mid-IR to THz region from GaSe crystal. The infrared-active modes of  $\epsilon$ -GaSe crystal at  $236\text{ cm}^{-1}$  and  $214\text{ cm}^{-1}$  were found to be responsible for the observed optical dispersion and infrared absorption edge. Based upon phase matching characteristics of GaSe for difference-frequency generation (DFG), new Sellmeier equations of GaSe were proposed. The output THz power variation with wavelength can be properly explained with a decrease of parametric gain and the spectral profile of absorption coefficient of GaSe. The adverse effect of infrared absorption on (DFG) process can partially be compensated by doping GaSe crystal with erbium ions.

©2006 Optical Society of America

**OCIS codes:** (190.4400) Nonlinear optics, materials; (190.2620) Frequency conversion; (320.7110) Ultrafast nonlinear optics, THz

---

## References and links

1. A. Bianchi and M. Garbi, "Down-conversion in the 4-18  $\mu\text{m}$  range with GaSe and AgGaSe<sub>2</sub> nonlinear crystals," *Opt. Commun.* **30**, 122-124 (1979).
2. K. L. Vodopyanov, L. A. Kulevskii, V. G. Voevodin, A. I. Gribenyukov, K. R. Allakhverdiev, and T. A. Kerimov, "High efficiency middle IR parametric superradiance in ZnGeP<sub>2</sub> and GaSe crystals pumped by an erbium laser," *Opt. Commun.* **83**, 322-326 (1991).
3. A. O. Okorogu, S. B. Mirov, W. Lee, D. I. Crouthamel, N. Jenkins, A. Yu. Dergachev, K. L. Vodopyanov, and V. V. Badikov, "Tunable middle infrared downconversion in GaSe and AgGaSe<sub>2</sub>," *Opt. Commun.* **155**, 307-312 (1998).
4. R. A. Kaindl, M. Wurm, K. Reimann, P. Hamm, A. M. Weiner, and M. Woerner, "Generation, shaping, and characterization of intense femtosecond pulses tunable from 3 to 20  $\mu\text{m}$ ," *J. Opt. Soc. Am. B* **17**, 2086-2094 (2000).
5. R. Huber, A. Brodschelm, F. Tauser, and A. Leitenstorfer, "Generation and field-resolved detection of femtosecond electromagnetic pulses tunable up to 41 THz," *Appl. Phys. Lett.* **76**, 3191-3193 (2000).
6. W. Shi, Y. J. Ding, X. Mu, and N. Fernelius, "Tunable and coherent nanosecond radiation in the range of 2.7-28.7  $\mu\text{m}$  based on difference-frequency generation in gallium selenide," *Appl. Phys. Lett.* **80**, 3889-3891 (2002).
7. K. Finsterbusch, A. Bayer, and H. Zacharias, "Tunable, narrow-band picosecond radiation in the mid-infrared by difference frequency mixing in GaSe and CdSe," *Appl. Phys. B* **79**, 457-462 (2004).
8. W. Shi and Y. J. Ding, "A monochromatic and high-power terahertz source tunable in the ranges of 2.7-38.4 and 58.2-3540  $\mu\text{m}$  for variety of potential applications," *Appl. Phys. Lett.* **84**, 1635-1637 (2004).

9. T. Tanabe, K. Suto, J. -i. Nishizawa, and T. Sasaki, "Characteristics of terahertz-wave generation from GaSe crystals," *J. Phys. D: Appl. Phys.* **37**, 155-158 (2004).
10. V. G. Dmitriev, G. G. Gurzadyan, and D. N. Nikogosyan, *Handbook of Nonlinear Optical Crystals* (Springer, Berlin, 1997), pp. 166-169.
11. N. B. Singh, D. R. Suhre, W. Rosch, R. Meyer, M. Marable, N. C. Fernelius, F. K. Hopkins, D. E. Zelmon, and R. Narayanan, "Modified GaSe crystals for mid-IR applications," *J. Cryst. Growth* **198**, 588-592 (1999).
12. S. Das, C. Ghosh, O. G. Voevodina, Yu. M. Andreev, and S. Yu. Sarkisov, "Modified GaSe crystal as a parametric frequency converter," *Appl. Phys. B* **82**, 43-46 (2006).
13. Y. -K. Hsu, C. -W. Chen, J. Y. Huang, C. -L. Pan, J. -Y. Zhang, and C. -S. Chang, "Erbium doped GaSe crystal for mid-IR applications," *Opt. Express* **14**, 5484-5491 (2006).
14. C. -L. Pan, C. -F. Hsieh, R. -P. Pan, M. Tanaka, F. Miyamaru, M. Tani, and M. Hangyo, "Control of enhanced THz transmission through metallic hole arrays using nematic liquid crystal," *Opt. Express* **13**, 3921-3930 (2005).
15. E. D. Palik, *Handbook of Optical Constants of Solids* (Academic, New York, 1998), Vol. III.
16. H. Yoshida, S. Nakashima, and A. Mitsuishi, "Phonon Raman Spectra of Layer Compound GaSe," *Phys. Status Solidi B* **59**, 655-666 (1973).
17. M. Hayek, O. Brafman, and R. M. A. Lieth, "Splitting and Coupling of Lattice Modes in the Layer Compounds GaSe, GaS, and GaSe<sub>1-x</sub>S<sub>x</sub>," *Phys. Rev. B* **8**, 2772-2779 (1973).
18. K. Allakhverdiev, T. Baykara, S. Ellialtioglu, F. Hashimzade, D. Huseinova, K. Kawamura, A. A. Kaya, A. M. Kulibekov (Gulubayov), and S. Onari, "Lattice vibrations of pure and doped GaSe," *Mater Res. Bull.* **41**, 751-763 (2006).
19. B. L. Yu, F. Zeng, V. Kartazayev, R. R. Alfano, and K. C. Mandal, "Terahertz studies of the dielectric response and second-order phonons in a GaSe crystal," *Appl. Phys. Lett.* **87**, 182104-1-3 (2005).
20. G. D. Boyd and D. A. Kleinman, "Parametric Interaction of Focused Gaussian Light Beams," *J. Appl. Phys.* **39**, 3597-3639 (1968).
21. K. L. Vodopyanov and L. A. Kulevskii, "New dispersion relationships for GaSe in the 0.65-18  $\mu\text{m}$  spectral region," *Opt. Commun.* **118**, 375-378 (1995).
22. K. R. Allakhverdiev, T. Baykara, A. K. Gulubayov, A. A. Kaya, J. Goldstein, N. Fernelius, S. Hanna, and Z. Salaeva, "Corrected infrared Sellmeier coefficients for gallium selenide," *J. Appl. Phys.* **98**, 093515-1-6 (2005).
23. T. J. Wieting and M. Schluter (Eds.), *Electrons and Phonons in Layered Crystal Structures* (D. Reidel Publishing Company, Holland, 1979), pp. 338-340.
24. R. A. Baumgartner and R. L. Byer, "Optical Parametric Amplification," *IEEE J. Quantum Electron.* **QE-15**, 432-444 (1979).

## 1. Introduction

Generation of broadly tunable coherent mid-infrared (mid-IR) pulses is of considerable interests in many disciplines ranging from molecular spectroscopy, bio-medical diagnostics, to remote sensing of atmospheric trace constituents. The most important technique to generate tunable coherent radiation in the mid infrared (mid-IR) is based on the second-order nonlinear optical (NLO) processes in a non-centrosymmetric crystal. These NLO processes include difference-frequency mixing, optical parametric generation and amplification [1-9].

The crystals used for mid-IR generation by frequency down conversion are still scarce and only a few of them have become commercially available [1-3]. Among these, GaSe is particularly attractive as it exhibits a fairly high effective nonlinear coefficient,  $d_{\text{eff}} = 54 \text{ pm/V}$  at  $10.6 \mu\text{m}$  and a wide transparency range from  $0.62 \mu\text{m}$  to  $20 \mu\text{m}$  [10]. It has been successfully employed for generation of coherent radiation in the mid-IR and even down to the THz frequency range by difference-frequency generation (DFG) or phase-matched optical rectification [5, 8]. Improvements in the optical nonlinearity of GaSe crystal with doping of silver or sulphur have been reported [11, 12]. Recently, we also reported that the nonlinear coefficient ( $d_{\text{eff}}$ ) of a GaSe crystal doped with 0.5 atom % erbium is 24% higher than that of a pure GaSe crystal [13].

GaSe is a semiconductor with layered hexagonal structure belonging to the  $D_{3h}^1 (P\bar{6}m2)$  space group. Beyond mid-IR, the infrared absorption edge of the NLO crystal places a practical limit on its frequency down conversion range. The infrared absorption edge of a crystal is usually attributed to infrared-active phonon modes or their combination modes. Unfortunately, there have been very limited studies concerning the effect of infrared absorption edge on the optical dispersion and frequency down conversion efficiency of NLO crystals, GaSe in particular.

In this work, we investigate the effect of infrared absorption on the generation properties of coherent infrared radiation from mid-IR to THz region using the GaSe crystal. Based upon the experimentally determined phase matching curves, modified Sellmeier equations of GaSe are proposed to more accurately describe the optical dispersion of this crystal in this spectral region. We identify the phonon modes that are responsible for the resulting infrared absorption edge. We also show that the absorption effect of these infrared active phonon modes can be reduced by doping GaSe crystal with erbium ions. The scheme increases the IR output and therefore extends the long wavelength tuning limit.

## 2. Experimental methods

The GaSe crystals used in this study were grown with the Bridgman method. For doped crystals or Er:GaSe, up to 0.5 atom % of erbium (99.95%) was introduced into the melt. Raw materials were placed in a well-cleaned quartz tube, sealed and then pumped down to below  $10^{-6}$  Torr. The crystal growth was carried out under a thermal gradient of 30 °C/cm with a growth rate of 2 cm/day. The resulting pure GaSe and Er:GaSe crystals exhibit the characteristic appearance of hexagonal layered structure of (001) plane. The crystal qualities were evaluated by measuring the X-ray rocking curve of the diffraction peak from the (008) plane. The optical transmission of the crystals were determined with a Fourier-transform infrared spectrometer (FTIR, Bomem DA8.3) in the mid-IR region and a home-made THz time-domain spectrometer (THz-TDS) [14] in the THz region, respectively. The crystal quality of the pure and the 0.5% Er:GaSe crystals are excellent. This is confirmed by measuring full-width-at-half-maximum (FWHM) widths of the (008) diffraction peaks, estimated to be about 0.02° and 0.025° for the pure and the 0.5% Er:GaSe crystals.

The GaSe difference-frequency generator (DFG) was implemented with a collinear type-I (o+o→e) phase-matching geometry. The pump beam of the DFG was provided by the fundamental output of an Nd:YAG laser ( $\lambda=1.064$   $\mu\text{m}$ ) with pulse duration of 20 ps, at a repetition rate of 10 Hz. The signal beam, with a pulse duration of 5 ps and tunable in the range of 1.1-1.8  $\mu\text{m}$  was generated by the idler output of a  $\beta$ -BaB<sub>2</sub>O<sub>4</sub> (BBO)-based optical parametric amplifier (OPA) pumped by the 355-nm output of the Nd:YAG laser. The typical pulse energy of the 1.064  $\mu\text{m}$  beam employed for DFG was about 750  $\mu\text{J}$ , while that of the OPA was adjusted between 35 and 50  $\mu\text{J}$ . The spot size of the pump beam was measured to be about 1.7 mm, corresponding to a maximum peak intensity of 1.7 GW/cm<sup>2</sup> on the GaSe crystal. The spot size of the signal beam after focusing is about 2.5 mm. In order to prevent optically induced damage, the samples are placed at the location of the focus of signal beam, which is before the focus of the pump beam. Both GaSe and the Er:GaSe crystals used in this study were not anti-reflection-coated and have a nominal thickness of 3.3 mm.

The generated mid-IR radiation was detected either with a cryogenically cooled mercury cadmium telluride (MCT) detector or a silicon bolometer. The residual pump radiation was blocked with a germanium (Ge) filter. The absolute pulse energies of the generated mid-IR radiation were determined with a calibrated pyroelectric detector. The generated pulse energies are corrected for the losses from Fresnel reflection and transmittance of the Ge filter.

## 3. Results and discussions

The absorption spectrum (see the solid curves) of the pure GaSe crystal from 5 to 1000  $\mu\text{m}$  is presented in Fig. 1. For comparison, the experimental data taken from Ref. [15] (filled symbols) and Ref. [9] (circles) are also included. A strong infrared absorption peak near 40–50  $\mu\text{m}$  (200–250 cm<sup>-1</sup>) can be clearly observed. Summarizing the lattice vibrational analysis and the existing data for infrared active phonons of  $\epsilon$ -GaSe [15], several longitudinal and transverse optical phonons modes were noticed to occur at 214 cm<sup>-1</sup> [E'(TO)], 237 cm<sup>-1</sup> (A<sub>1</sub>') and 255 cm<sup>-1</sup> [E'(LO)]. Before the absorption edge, some other IR-active modes at 19.6  $\mu\text{m}$  (510 cm<sup>-1</sup>), 22.4  $\mu\text{m}$  (446 cm<sup>-1</sup>), 24.4  $\mu\text{m}$  (410 cm<sup>-1</sup>), 27.6  $\mu\text{m}$  (362 cm<sup>-1</sup>), 30.4  $\mu\text{m}$  (329 cm<sup>-1</sup>), and 33.1  $\mu\text{m}$  (302 cm<sup>-1</sup>) can also be identified. These modes are assigned as the difference-frequency combinations of acoustic and optical phonons or the impurity-induced localized

modes. For example, the band at 24.4  $\mu\text{m}$  is the overtone of the IR active mode at 46.7  $\mu\text{m}$ . The band at 27.6  $\mu\text{m}$  has its origin from the multi-phonon processes, while the two bands at 19.6  $\mu\text{m}$  and 22.4  $\mu\text{m}$  are mainly due to the impurity-induced localized modes [16-19]. The pre-edge IR absorption of  $\text{Er}^{3+}:\text{GaSe}$  is lower than that of pure crystal because the linear chain structure of  $\text{Se-Ga-Ga-Se-Se-Ga-Ga-Se}$  [13] in pure GaSe crystal is disrupted by erbium dopants. As a result, the induced vacancies or substitutional impurities in GaSe crystal are shifted to lower frequencies. Consequently, the heights of overtone absorption peaks from the unperturbed part of GaSe lattice are reduced.

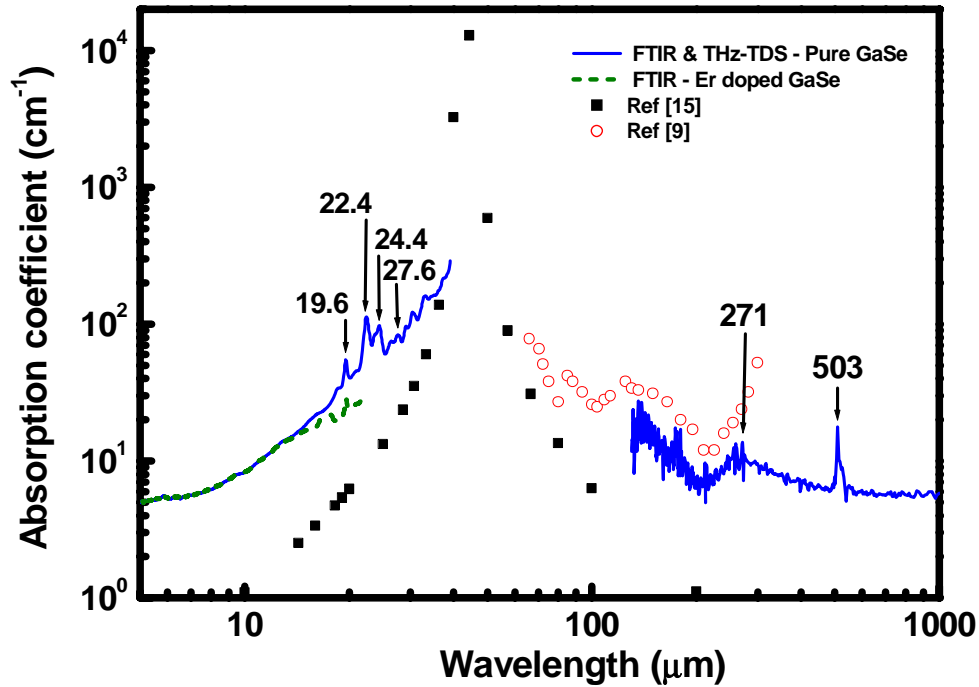


Fig. 1. Absorption coefficients of GaSe are plotted as a function of wavelength in the mid-IR and far-IR. The filled squares and open circles are data taken from Refs. [15] and [9], respectively. The solid curves show our experimental results measured by FTIR and THz-TDS for pure and  $\text{Er}^{3+}:\text{GaSe}$

Two absorption peaks at 271  $\mu\text{m}$  ( $37\text{ cm}^{-1}$ ) and 503  $\mu\text{m}$  ( $20\text{ cm}^{-1}$ ) in the THz region are attributed to an interlayer vibration of GaSe with  $A_1$ - and  $E'$ -type symmetries, respectively [16, 17]. The presence of the low-frequency sharp peak of “rigid layer mode” at  $20\text{ cm}^{-1}$  indicates our pure GaSe crystal to be in the  $\epsilon$ -phase. The broader feature at  $37\text{ cm}^{-1}$  is associated with collective interlayer motion along the  $z$ -axis of GaSe involving multiple rigid layers. The absorption coefficients in the 130–270  $\mu\text{m}$  range measured by THz-TDS exhibits an enhanced transmission near 200  $\mu\text{m}$ , which is in agreement with that reported in Ref. [9]. The typical interlayer distance of a GaSe crystal is about a few tens of micrometers. The increasing transmission could therefore originate from the destructive interference effect of multiple reflections in the Fabry-Perot cavity of GaSe layers with slightly irregular distribution of interlayer distances.

We have measured the conversion efficiency for second-harmonic-generation (SHG) from a pure GaSe crystal excited with a pump wavelength of 6  $\mu\text{m}$  [13]. This is plotted as a

function of the pump energy in the inset of Fig. 2. At each pump energy, the measurement was conducted a number of times to reveal the fluctuation range of the data. The type-I ( $o+o\rightarrow e$ ) phase-matching condition is satisfied with an external phase-matching angle of  $30.2^\circ$ . Following *Boyd and Kleinman* [20] and using the slope of the SHG conversion efficiency, we have determined the nonlinear coefficient  $d_{22}$  of the pure GaSe crystal to be 56 pm/V, which agrees well with a value of 54 pm/V reported in Ref. [10].

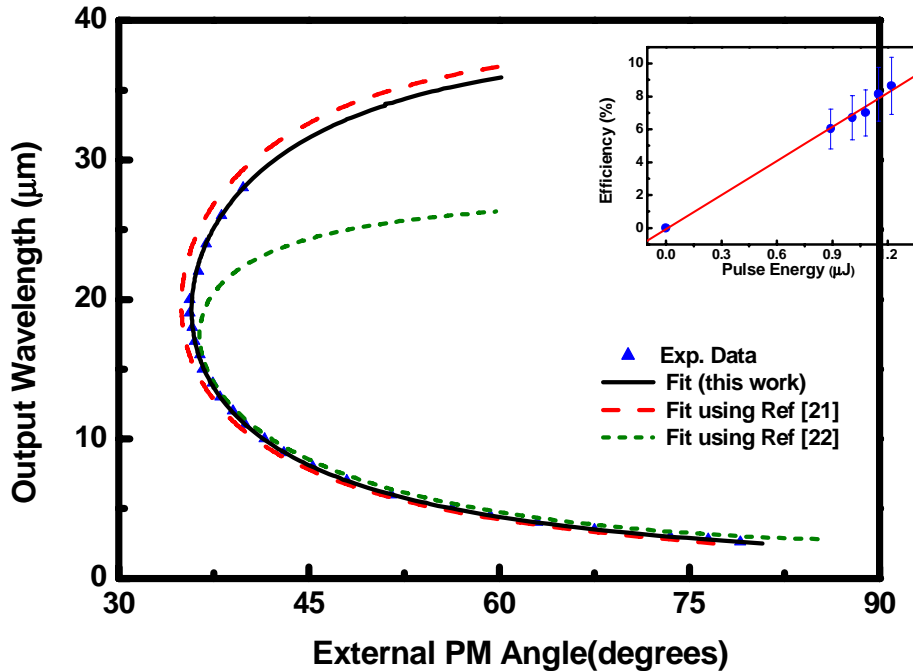


Fig. 2. Type-I DFG output wavelength vs. external PM angle. The filled triangles show the experimental data and solid curve is the fitting curve using the modified Sellmeier equation. Dashed curve: calculated phase matching curve using dispersion of GaSe from Ref. [21]. Dotted curve: calculated phase matching curve using dispersion of GaSe from Ref. [22]. Inset: Measured SHG efficiency of a 3.3-mm long GaSe crystal as a function of the internal pulse energy

The tuning curve of a collinear type-I phase-matched GaSe DFG pumped at  $1.064\ \mu\text{m}$  is presented in Fig. 2. The filled triangles in Fig. 2 are the experimental data. The broken lines in red and green are the calculated results by using the Sellmeier equations reported in Ref. [21] and Ref. [22], respectively. To characterize the phase matching (PM) curves, we prepare one sample for each type of GaSe crystals. We first carefully determine the crystal orientation with a zero external angle. The phase matching angles can be measured with an accuracy limited by the rotational stage used. The tuning curves are highly reproducible for different measurement runs with each data point having a measurement accuracy of  $\pm 0.2^\circ$  in crystal orientation and 10 nm in wavelength. The difference between the phase matching tuning curves of the pure GaSe and the Er:GaSe (not shown here) can not be distinguished within the measurement accuracy. The Erbium doping appears to produce very small perturbation on the lattice of GaSe and therefore its role can not be revealed in the Sellmeier equations and PM curve.

The tuning curves shown in Fig. 2 indicate that by varying the external PM angle from 34° to 80°, the DFG output can be tuned from 2.4 to 28 μm. For the output wavelengths longer than 20 μm, however, the experimental PM angles show significant deviation from the two calculated phase matching curves. Compared to the curve with Sellmeier equations taken from Ref. [21], our measured data points deviate from the calculated curve by 2%–4% (0.7°–3.3°), which are larger than the error bar of our experimental data. A uniform shift of the measured data along the x-axis, which results in a deviation of 0.6°–2.6°, can not yield a satisfactory fit to the PM curve from Ref. [21]. Furthermore the absolute crystal orientation with a zero external angle can be measured to rule out this possibility. Therefore, to fit the PM curve for DFG satisfactorily, we propose the following modified Sellmeier equations for GaSe.

For o-ray,

$$n_o^2 = A + \frac{B}{\lambda^2} + \frac{C}{\lambda^4} + \frac{D}{\lambda^6} + \frac{E\lambda^2}{\lambda^2 - F}, \quad (1)$$

where  $\lambda$  is the wavelength in micrometers, and  $A=6.8517$ ,  $B=0.4558$ ,  $C=0.0143$ ,  $D=0.0043$ ,  $E=3.6187$ ,  $F=2210.7$ . Similarly, the modified Sellmeier equation for e-ray is given by

$$n_e^2 = A' + \frac{B'}{\lambda^2} + \frac{C'}{\lambda^4} + \frac{D'}{\lambda^6} + \frac{E'\lambda^2}{\lambda^2 - F'}, \quad (2)$$

with  $A' = 5.187$ ,  $B' = 0.4634$ ,  $C' = -0.232$ ,  $D' = 0.1083$ ,  $E' = 1.8105$ , and  $F' = 1801.65$ . The modified Sellmeier equations are expected to be accurate in the spectral range of 2.4–35 μm and had been experimentally verified from 2.4 to 28 μm.

The phase matching curve based our modified Sellmeier equations is plotted in Fig. 2 as the solid curve. Excellent agreement with experimental data points is achieved. The improvement of our fit with Eqs. (1) and (2) from that with Ref. [21] is statistically significant, implying that our modified Sellmeier equations can be used to yield useful information about the lattice vibrations responsible for the absorption edge. There have been very limited studies concerning the origin and effect of infrared absorption edge on the optical dispersion of a NLO crystal. The information reported is crucial in view that infrared absorption edge is an important parameter for the design of new infrared NLO crystals.

The poles of the modified Sellmeier equations occur at 42.4 μm for the e-ray and 47 μm for the o-ray, respectively. The pole of the o-ray dispersion corresponds to an infrared active mode of  $E'$ -symmetry with vibration involving both Ga and Se atoms on the basal plane of GaSe crystal. The optical field of the o-ray propagating through the GaSe crystal thus experiences an index of refraction reflecting the intralayer covalent bonding structure of GaSe. The pole of the e-ray dispersion corresponds to an infrared active mode of  $A_2''$ -symmetry with vibration involving both Ga and Se atoms along the optical axis (c-axis). The optical field of the e-ray then experiences an index of refraction, reflecting an optical dispersion from the interlayer vibration in the GaSe crystal [23].

The parametric gain can be written as [24]

$$\Gamma(\lambda) = \sqrt{\frac{8\pi^2 d_{\text{eff}}^2 I_p}{\epsilon_0 c n_s n_i n_p \lambda_s \lambda_i}}, \quad (3)$$

where  $I_p$  is the intensity of the pump beam;  $d_{eff}$  is the effective nonlinear coefficient;  $\epsilon_0$  is the permittivity of free space;  $c$  is the light velocity in vacuum;  $n_p, n_s, n_i$  correspond to the indices of refraction at the pump, the seeding and the generated IR wavelengths;  $\lambda_s$  and  $\lambda_i$  correspond to the wavelengths of the seeding and the idler IR pulses, respectively.

The theoretical parametric gain and absorption coefficients of pure GaSe are plotted as a function of wavelength in Fig. 3(a). The output pulse energies of a 3.3-mm-long pure GaSe DFG from 2.4–28  $\mu\text{m}$  are presented as solid squares in Fig. 3(b). The energy of the infrared pulses generated at 3.5  $\mu\text{m}$  was about  $\sim 13 \mu\text{J}$  with a photon conversion efficiency of 7.3%. This DFG system has stable output with  $\pm 8\%$  power fluctuation, which is due mainly to the fluctuation of the laser and is treated as the error bars in the measurement. With the exception of the absorption band around 40–50  $\mu\text{m}$ , the output pulse energy decreases monotonically with increasing wavelength. This is attributed to a decrease in parametric gain and an increase in linear absorption loss of GaSe crystal.

The generation of infrared pulses via down conversion can be modeled with a parametric amplification process under a depleted pump beam condition [24]:

$$I_i(r) = \left[ \left( \frac{\omega_i}{\omega_p} \right) I_p (1 - sn^2[(r - r_0)/l, r]) \right] \times \exp(-\alpha r), \quad (4)$$

where

$$1/l = \Gamma(\lambda) \sqrt{1 + \frac{I_s \omega_p}{I_p \omega_s}}, \quad (5)$$

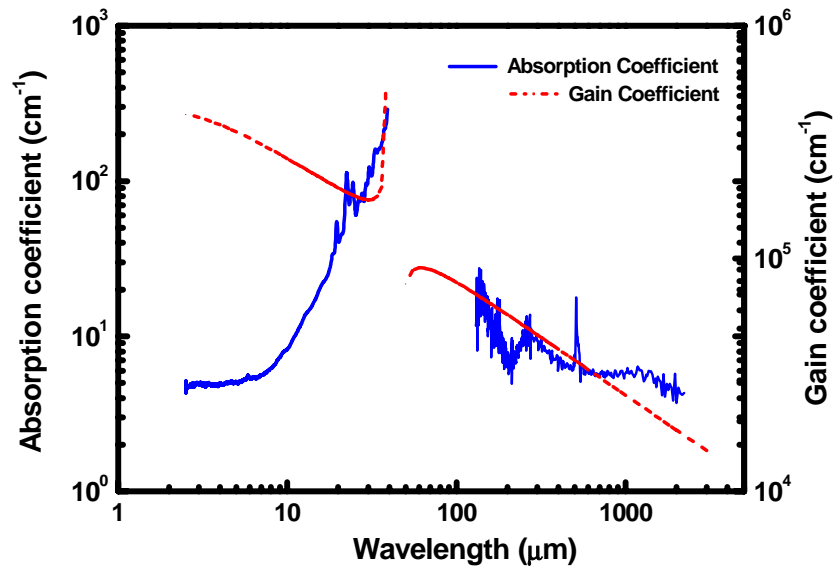
and

$$r_0/l = \frac{1}{2} \ln \left( 16 \left[ 1 + \frac{I_p \omega_s}{I_s \omega_p} \right] \right). \quad (6)$$

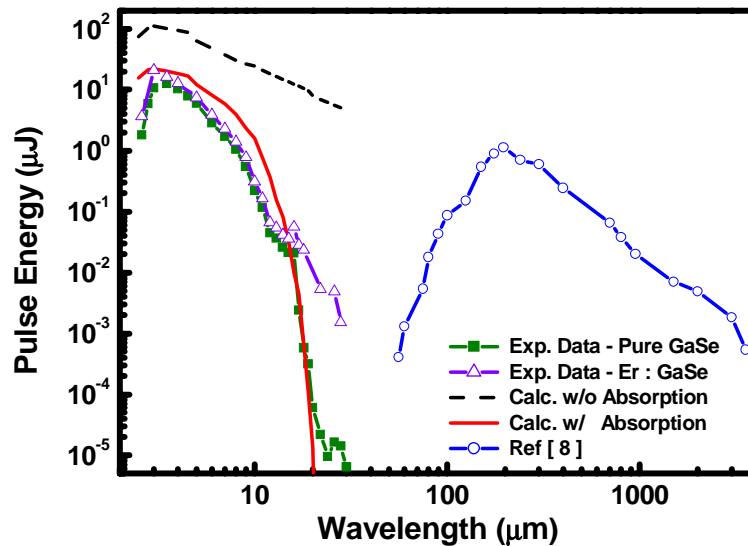
In Eqs. (4)–(6),  $I_p$  is the pump intensity;  $I_s$  is the seeding intensity;  $\Gamma(\lambda)$  is the parametric gain coefficient;  $\alpha$  is the absorption coefficient;  $\omega_j$ ,  $j = p, s, \text{ or } i$  is the angular frequency of the pump, the seeding and the IR pulses, respectively;  $r$  is length of the GaSe crystal. We note that  $sn$  in Eq. (4) is the Jacobian elliptic function resulting from an inversion operation of the elliptic integral [24].

By taking into account the experimentally determined temporal and spatial profiles of the laser pulses, the calculated output pulse energy without considering loss due to absorption in the crystal is presented as the dashed curve in Fig. 3(b). The theoretical prediction taking into account the loss is shown as the solid curve. Clearly the solid curve exhibits better agreement with the experimental data. This reflects significant effect of infrared absorption of GaSe on the DFG output. The Er:GaSe DFG generated higher output pulse energy than the pure GaSe DFG near 20  $\mu\text{m}$ , as shown by the open triangles in Fig. 3(b). This is attributed to lower absorption loss of Er:GaSe near 20  $\mu\text{m}$  as well as an increased second-order optical nonlinearity from erbium doping [13].

For comparison, the wavelength-dependent output data in THz region [see the open circles in Fig. 3(b)] are taken from the data reported by *Shi et al.* [8]. Notice that the output THz radiation peaks at a wavelength of 200  $\mu\text{m}$ , which overlaps with the enhanced transmission region shown in Fig. 1. After reaching the maximum, the output pulse energy decreases with increasing wavelength. This is mainly due to a decrease in parametric gain.



(a)



(b)

Fig. 3. (a) Calculated parametric gain (dashed curve) and measured infrared absorption (solid curve) as a function of wavelength. (b) Measured and calculated pulse energies of the DFG generator versus wavelength. Solid squares show the measured infrared pulse energies for pure GaSe, open triangles show the measured infrared pulse energies for  $\text{Er}^{3+}$ :GaSe, solid curve and dashed curve indicate the calculated pulse energies with and without considering the crystal linear absorption coefficient, respectively. The open circles shown in the THz region are taken from Ref. [8] for comparison.



#### **4. Conclusions**

We report a study of the effect of optical absorption on generation of coherent infrared radiation from mid-IR to THz region from GaSe crystal. The infrared-active modes of  $\epsilon$ -GaSe crystal at  $236\text{ cm}^{-1}$  and  $214\text{ cm}^{-1}$  were found to be responsible for the observed optical dispersion and infrared absorption edge. Based upon phase matching characteristics of GaSe for difference-frequency generation (DFG), new Sellmeier equations of GaSe were proposed. The output THz power variation with wavelength can be properly explained with a decrease of parametric gain and the spectral profile of absorption coefficient of GaSe. The adverse effect of infrared absorption on (DFG) process can partially be compensated by doping GaSe crystal with erbium ions.

#### **Acknowledgments**

Ching-Wei Chen would like to thank Cho-Fan Hsieh for assistance in taking the THz-TDS data. This work was supported by the National Science Council of the Republic of China, Taiwan under Contracts No. 89-E-FA06-AB, NSC94-2112-M-009 -033, and PPAEU-II. The authors are also sponsored by the ATU Program of the Ministry of Education, the Republic of China.